

Out of step condition and torsional stress of synchronous generators

Alessandro Manunza
M2EC, Italy

M2EC
Via Coppelli, 15
20037, Paderno Dugnano (MI), Italy
manunzaalessandro@tiscali.it

Abstract - *Out-of-step operation of synchronous generators causes torsional and electro-magnetic stresses. The aim of the paper is to compare three of the most used out-of-step protection algorithms, to find out some qualitative indications for protection setting and to evaluate the limits on these algorithms. Electrical and mechanical components and protections have been modeled in ATP and subjected to several fault conditions. The study demonstrates that these algorithms should adapt the clearing time according to the fault location. The next generation of algorithms should consider not only the impedance loci but also the torsional oscillations and their consequences on the generator voltage.*

Keywords: *Synchronous generator, out of step condition, torsion, protection, sub-synchronous oscillations*

1 Introduction

The out-of-step condition of synchronous generator is cause of torsional stress for the mechanical system and of electro-magnetic stress for the generator circuit breaker. Therefore a proper setting of the out-of-step (ANSI type 78 device) protection should reduce these stresses, but the choice of this is never a simple task, even in those cases in which the transient stability study is available. Moreover different relays may implement different algorithms and technical literature reports some typical characteristic curves drawn on the impedance locus: single blinder, double blinder, rectangular, lens, “tomato” shapes. The aim of this study is to compare some of the most used algorithms, to find out some qualitative indications for the protection setting in order to reduce mechanical stresses and for the choice of the protection curve.

2 “Out of Step” condition

Power system faults, line switching, generator disconnection, and the loss or application of large blocks of load result in sudden changes to electrical power, whereas the mechanical power input to generators remains relatively constant. The loss of equilibrium between the produced and the consumed power causes the acceleration of the rotating masses of synchronous generators. Depending on the severity of the disturbance and the actions of power

system controls, the system may or may not return to a new equilibrium state. The condition under which one or more machines lose synchronism with other machines connected to the same grid is known as “out of step” or “pole slip”.

Prolonged “out of step” condition can have the following consequences:

1. Cyclic fluctuation in voltage can dramatically affect rotating machines;
2. Several kinds of relays may operate improperly;
3. Shafts of the synchronous machines are subject to torsional stresses.

Generally a rotating shaft is mainly composed by a prime mover rotor and a generator rotor and during an “out of step” condition, the prime mover maintains almost constant the torque applied to its rotor, while the electrical torque varies. Thus the rotating shaft faces torsional stresses and fatigue that can reach a critical condition like that shown in figure 2-1.



Fig. 2-1. Shaft crack caused by an out-of-step condition.

3 The analysed system

In this chapter the system under examination will be described with detail on the electrical system, the mechanical system and the protection relay.

3.1 The electrical system

The analysed electrical system, shown in figure 3-1, is composed by a synchronous generator, a step-up transformer, a HV line and an equivalent generator. The data of the components are as follows:

Equivalent Generator	
Rated Voltage (kV)	220
Rated Power (MVA)	8500
No. of poles	2
$X_d = X_q$ (%)	200
$X'_d = X'_q$ (%)	100
$X''_d = X''_q$ (%)	90
T'_{do} (s)	10
T'_{qo} (s)	1
$T''_{do} = T''_{qo}$ (s)	0.1
J ($10^6 \text{ kg}\cdot\text{m}^2$)	0.5166

Step Up transformer	
Rated Voltage (kV)	225/15.75
Rated Power (MVA)	320
Vector Group	YNd11
Resistance (%)	0.22
Reactance (%)	13
Magn. Current (%)	0.32
Pfe (kW)	200

HV Line	
Rated Voltage (kV)	220
Length (km)	100
R_1 (ohm/km)	0.024
X_1 (ohm/km)	0.201
C_1 (nF/km)	11

Generator			
V_r (kV)	15.75	X'_d (pu)	0.185
A_r (MVA)	318.3	X''_q (pu)	0.185
$\cos\Phi$	0.9	X_c (pu)	0.16
R_a (pu)	0.0024	X_o (pu)	0.135
X_l (pu)	0.16	T'_{do} (s)	6.4
X_d (pu)	2.23	T'_{qo} (s)	0.59
X_q (pu)	2.14	T''_{do} (s)	0.44
X'_d (pu)	0.26	T''_{qo} (s)	0.086
X'_q (pu)	0.82	J (kg m^2)	see below

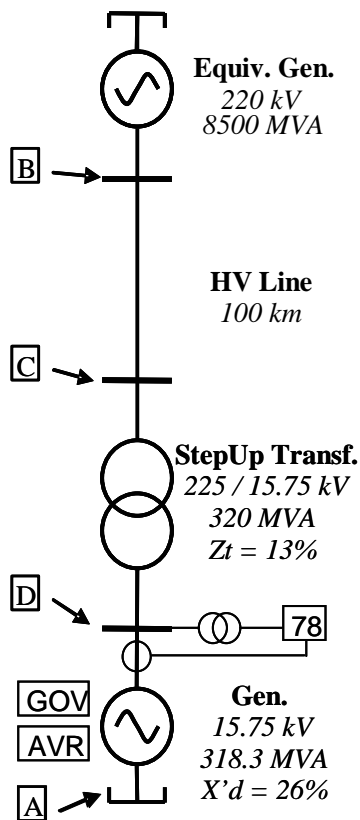


Fig. 3-1. Simplified single line diagram.

The generator is equipped with the speed governor and the voltage regulator.

The speed governor is a typical controller for gas turbine, which regulates the gas injection with a PI controller to make null the error of the mechanical frequency.

The automatic voltage regulator (AVR) is represented as indicated by the ST4B model of the IEEE 421.5-2005 standard. The PSS is represented by the PSS2B model of the same standard.

The characteristic impedances of the system can also be represented in the (R, X) plane as indicated in figure 3-2. Each component is represented by its impedance as measured by the relay at the generator terminals. Please note that the scales of the two axes are different.

The whole system can be represented by the segment AB.

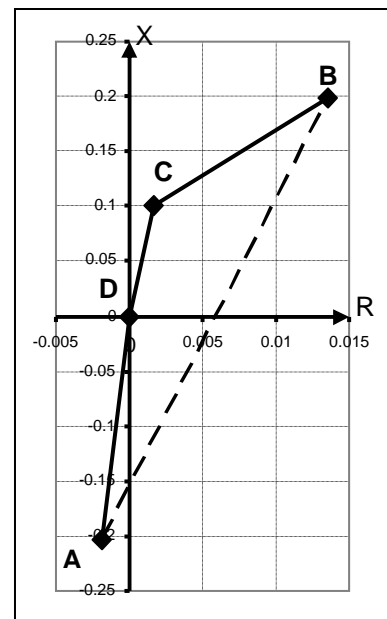


Fig. 3-2. System impedances.

Segment	Component	R (ohm)	X (ohm)
AD	Generator	0.0019	0.203
DC	Transformer	0.0017	0.1008
CB	OH Line	0.0118	0.098

3.2 The mechanical system

3.2.1 The real system

Mechanical data of the rotating system have been extracted from [10]. The rotating shaft of the generator consists of the generator rotor, the load coupling and the gas turbine. The operating speed of the system is 3000 rpm. Figure 3-3 shows a representation of the rotating system.

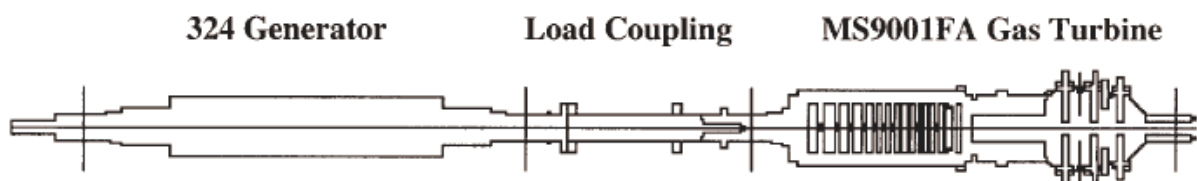


Fig. 3-3. Mechanical arrangement.

The mechanical data of the rotating system are:

	Generator	Coupling	Turbine
Shaft Length (m)	10.54	2.2	10.02
Inertia J (kg m ²)	4796.7	234.4	30876.1
Shear Modulus G (Pa)	7.93x10 ¹⁰	7.72x10 ¹⁰	7.52x10 ¹⁰

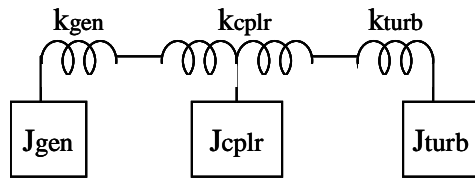
The natural frequencies of torsional oscillations are 22.7 Hz, 102.7 Hz, 144.4 Hz and 196.2 Hz, as indicated in the report of the rotor-dynamical analysis [10].

3.2.2 The model

This complex mechanical system has been modelled as composed by three masses and two springs, as illustrated in figure 3-4.

Each rotor can be considered as a rotating mass plus a torsional spring, whose equation is:

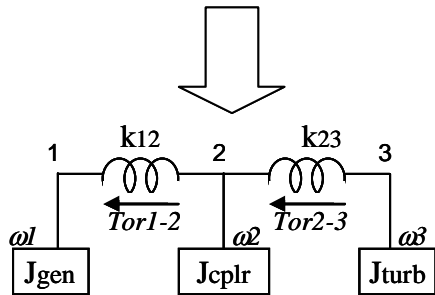
$$T = k \times \Delta\vartheta \quad \text{Eq. 1}$$



where
 T = torsional torque
 $\Delta\theta$ = angle displacement between the two ends
 k = shaft stiffness

The shaft stiffness has been calculated as each rotor were a cylinder. Thus

$$k = \frac{G J_p}{L} = \frac{G \pi D^4}{32L} \quad \text{Eq. 2}$$



where
 G = shear modulus
 D = diameter
 L = length

Fig. 3-4. Mechanical model.

Moreover the equivalent spring of the coupler has been subdivided into two identical parts, that have been associated to the generator and turbine springs respectively.

The inertia moment of the coupler has been increased by 9 times in order to obtain the resonance frequencies of the real rotating system. However the inertia of the whole rotating system has been increased of only 5%. The data of the equivalent model are reported in the following table.

	Generator	Coupling	Turbine
Estimated Shaft Diameter (m)	0.55	0.35	1
Polar moment J_p (m ⁴)	8.98x10 ⁻³	1.47x10 ³	9.82x10 ²
Stiffness $k=G*J_p / L$	6.76x10 ⁷	5.17x10 ⁷	7.37x10 ⁸
Inertia J (kg m ²)	4796.7	2191.8	30876.1

The maximum shear stress that steel can withstand is about $\tau_{adm} = 4 \times 10^8$ Pa.

In a cylinder the maximum torsional stress is located on the external circumference, so the maximum admissible torque can be calculated with the following equation:

$$\tau_{adm} = \frac{16T_{adm}}{\pi D^3} \quad \text{Eq. 3}$$

The following table reports the maximum admissible torque estimated for each component of the rotating shaft.

	Generator	Coupling	Turbine
Estimated Shaft Diameter (m)	0.55	0.35	1
Admissible torque (Nm)	1.3×10^7	3.4×10^6	7.85×10^7

Damping effects have been neglected because of their limited consequences on the analysed phenomena.

3.3 Electrical protection

The aim of the “out of step” protection, in the following indicated with its ANSI code 78, is to disconnect the synchronous generator when a pole slip is detected.

Most of “78” relays are based on the measurement of impedance and its variation in time. A relay operates only if the electrical centre P between the machine and the rest of the system passes through the protected zone. The protected zone is represented by the segment AB of figure 3-2 and repeated in figure 3-5.

Relays may implement different kinds of algorithms to detect the pole slip condition. These algorithms can be represented on the (R,X) plane by different curves, whose shapes give the name to the algorithms: single blinder, double blinder, rectangular, lens, “tomato”. All these algorithms produce a relay trip after a pole slip occurs.

In this work, the single blinder, lens and tomato shapes have been analysed and compared.

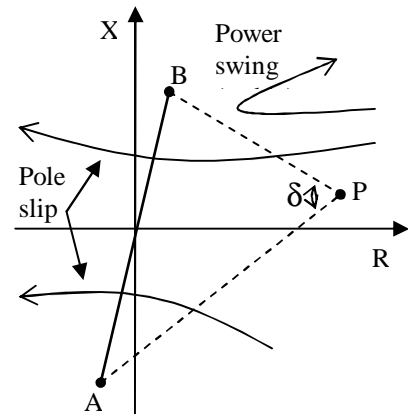


Fig. 3-5. Typical impedance loci.

3.3.1 Single blinder

The single blinder characteristic is composed by two straight lines, which are parallel to the AB segment. The relay tripping occurs whenever the electrical centre P crosses both lines. In case of stable power swings, nothing happens.

The characteristic is determined when three parameters are known: the points A and B and the X-intercept of the straight line α .

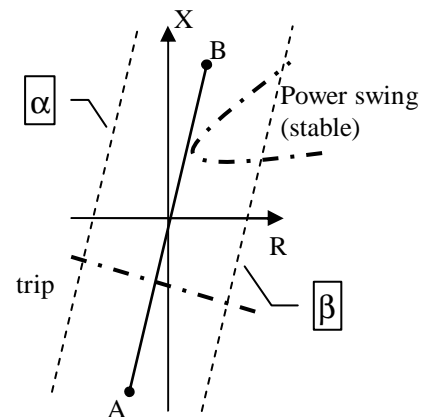


Fig. 3-6. Single blinder characteristic.

3.4 Lens shape

This characteristic consists of two arcs α_1 , α_2 as shown in figure 3-7. It is completely determined by three elements: point A, point B and angle γ .

Whenever the electrical centre enters in α_1 and exists from α_2 , the relay trips. In case of stable power swings, nothing happens.

This curve is usually shown with an angle γ almost equal to 120° .

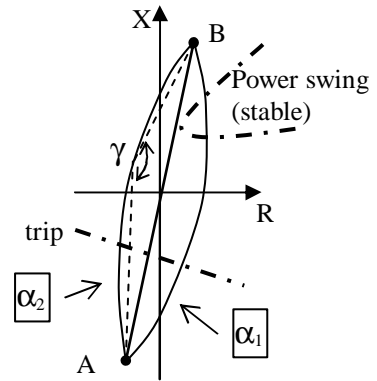


Fig. 3-7. Lens characteristic.

3.5 Tomato shape

This algorithm requires five parameters: two point (A and B), two angles (γ_1 and γ_2) and a time interval (Δt), as shown in figure 3-8. The relay trips whenever the electrical centre crosses the space between the outer and inner curves in a time interval greater than Δt . Thus the relay trips if ($\Delta t_{12} > \Delta t$) OR ($\Delta t_{34} > \Delta t$). In this way the relay trips also if a stable power swing crosses curves α_1 and α_2 as indicated in the right top corner of the figure 3-8. In this study only curves α_1 and α_2 have been considered.

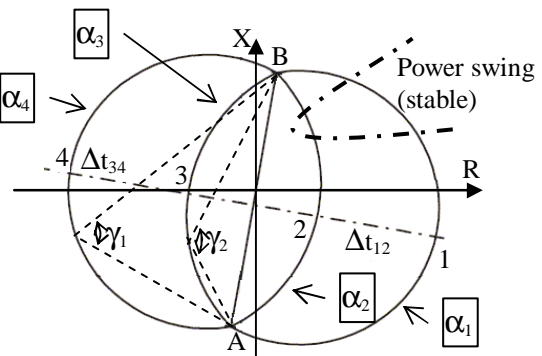


Fig. 3-8. Tomato characteristic.

4 Modelling and Simulation

4.1 Modelling with ATPDraw

The electrical components have been simulated as follows:

- The equivalent generator has been modelled with a “SM59_NC” component;
- The HV line has been modelled with four “LINEPI3S” components, which may be considered suitable for electromechanical transient studies;
- The step-up transformer has been modelled with a “BCTRAN3” component;
- The generator circuit breaker has been modelled with three “TACS-controlled TYPE 13” switches;
- The synchronous generator has been modelled with a “SM59_FC” component, which makes eight internal variables available.

The whole system is shown in figure 4-1.

TACS have been used in modelling AVR, PSS and Governor, while MODELS language has been used for the simulation of the 78 relay.

4.2 Modelling with ATP

ATPDraw does not allow modelling of a multi-mass rotor of a synchronous generator with a “SM59_FC” component. The mechanical model of the rotating shaft has been input directly in the ATP file. The generator was modelled as reported here below:

```

C < n 1><> < Ampl. >< Freq. ><Phase/T0>< A1 >< T1 >< TSTART >< TSTOP >
59GENA      12859.      50.      41.59
  GENB
  GENC
PARAMETER FITTING      3.
3 1 1 2      1.      1.      318.3      15.75      1600.
BLANK
C Ra >> Xl >> Xd >> Xq >> X'd >> X'q >> X''d >> X''q >
.0024      .16      2.23      2.14      .26      .82      .185      .185
C T'do >> T'qo >> T''do >> T''qo >> Xo >> Rn >> Xn >> Xc >
6.4      .59      .044      .086      .135      .16
C Class 4 S.M. data Card
C 1=Generator 2= Coupler 3= Gas Turbine
C ML> < EXTRS >< HICO >< DSR >< DSM >< HSP >< DSD >
1      0.0      .00480      0.0      0.0      93.43      0.0
2      0.0      .00219      0.0      0.0      762.64      0.0
3      1.0      .03088      0.0      0.0      0.0      0.0
BLANK
10
21
31
41
50
BLANK
73IFD      4
72PMECH      1
74WMECH      2
71EF
FINISH

```

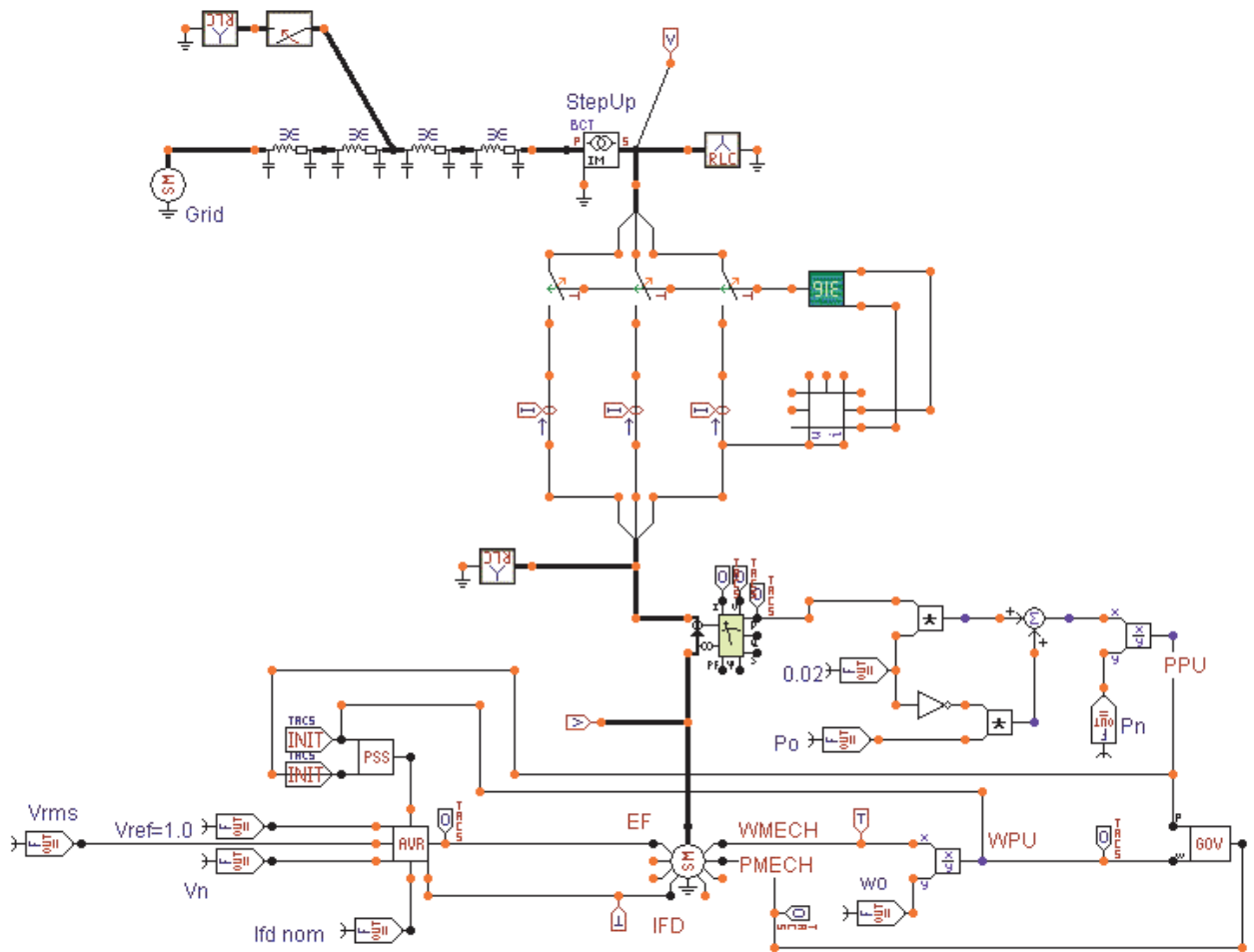


Fig. 4-1. ATPDraw model of the whole system.

4.3 “Out of Step” relay

The algorithm of the relay 78 is based on the capacity to determine if the electrical centre is inside or outside the characteristic curve.

4.3.1 Single blinder

Whenever the electrical centre of the system, indicated by the point P in figure 4-2, is at the left of the left blinder, then the relay must trip. The tripping condition is:

$$X_p > mR_p + q \quad \text{Eq. 5}$$

The relay has been simulated by means of the MODELS language.

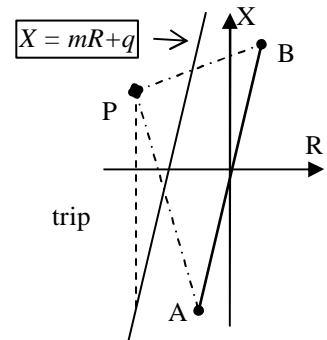


Fig. 4-2. Single blinder tripping condition.

4.3.2 Lens and tomato shape

The lens shape and tomato shape characteristic curves are composed by arcs of circumferences. Thus the point P is inside the arc and at the left of the segment AB if the following condition holds:

$$\{[(m_A < m_{tgA}) \text{ OR } (m_A > m)] \& (d < r)\} \quad \text{Eq. 6}$$

Otherwise the point P is outside the curve and at the left of the segment AB if the following equation is true:

$$\{[(R_p > R_A) \& (m_A > m)] \text{ OR } [(R_p < R_A) \& (m_A < m)]\} \& (d > r) \quad \text{Eq. 7}$$

Please refer to figure 4-3 for the meaning of the symbols.

Based on these equations, the relay has been simulated by means of the MODELS language. The self-explaining source code for the lens curve has been reported below. The source code for the tomato shape relay is more complex because the crossing time has also been calculated.

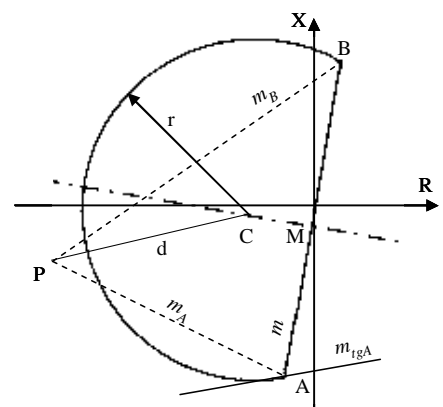


Fig. 4-3. Lens characteristic.

```

MODEL LENS
INPUT
  r                -- Actual Resistance
  x                -- Actual Reactance
DATA
  rA              -- Resistance point A
  xA              -- Reactance point A
  rB              -- Resistance point B
  xB              -- Reactance point B
  gamma          -- angle in degrees
  cbdela {DFLT:0.05} -- breaking time of the cb in seconds
VAR
  a b gamrad m mA rM xM h radius
  rC xC ml mtgA dist p q s intern estern trip condiz
OUTPUT
  trip
HISTORY
  condiz          {dflt: 0}
DELAY CELLS (condiz): cbdela/timestep + 1

INIT
-- Building of the tripping curve

```



```

gamrad := gamma *pi/180
m := (xB-xA)/(rB-rA)
rM := (rA+rB)/2
xM := (xA+xB)/2
h := sqrt( (rB-rM)*(rB-rM) + (xB-xM)*(xB-xM) )
radius := h / sin(gamrad)
m1 := -1/m
b := xM + rM/m
p := 1+ m1*m1
q := 2*(m1*b - rB - m1*xB)
s := rB*rB + xB*xB + b*b - radius*radius - 2*xB*b
if (gamma < 90) then
  rC := (-q-sqrt(q*q-4*p*s))/(2*p)
else
  rC := (-q+sqrt(q*q-4*p*s))/(2*p)
endif
xC := m1*rC+b
mCA := (xC-xA)/(rC-rA)
mtgA := -1/ mCA
-- parameters initialization
mA := 0.0
intern := 0.0
estern := 1.0
trip := 1.0
condiz := 1.0
ENDINIT
EXEC
-- determine the P position
mA := (x - xA)/(r - rA)
dist := sqrt( (r-rC)*(r-rC) + (x-xC)*(x-xC) )
-- Is it external?
a := and((r < rA), (mA < m))
b := and((r > rA), (mA > m))
estern := and( or(a,b), (dist > radius) )
-- If it was internal and now is external then the tripping conditions are true
if and(intern, estern) then
  condiz := 0.0
endif
-- Is it internal?
intern := and( or((mA < mtgA), (mA > m)), (dist < radius) )
-- If the circuit breaker delay is elapsed then trip
if (t > cbdela) then
  trip := delay(condiz, cbdela)
endif
ENDEXEC
ENDMODEL

```

5 Initial transient

The cause of the “out of step” condition to be studied is a 3 phase short circuit at a fixed point of the HV line. The short circuit starts at $t = 0.05$ ms and not at $t = 0$, in order to verify the pre-fault steady state. For the sake of the analysis here proposed, the fault must last enough time to guarantee that the generator rotor has accelerated so much that the pole slip occurs even after the fault is cleared.

In the analysis of this initial transient, four different fault clearance times have been considered, namely 380 ms, 390 ms, 400 ms and 410 ms. All these clearance times are longer than the usual values on HV line protections.

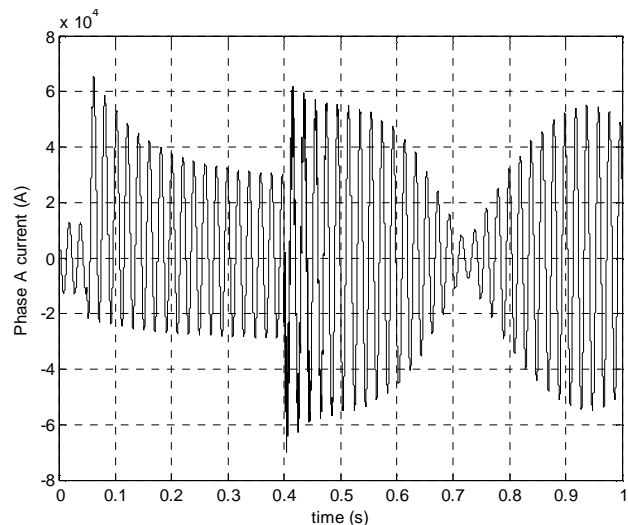


Fig. 5-1. Generator current in phase A .

Figure 5-1 shows the generator current of phase A in case of fault clearance at $t = 400$ ms, where it is possible to distinguish the pre-fault current ($0 < t < 50$ ms), the typical trend of the fault current ($50 < t < 400$ ms) and the current of the out of step condition ($t > 400$ ms).

In figure 5-2, the time behaviour of R and X is reported as measured at the generator terminals. The same quantities are reported in a (R,X) plane in figure 5-3.

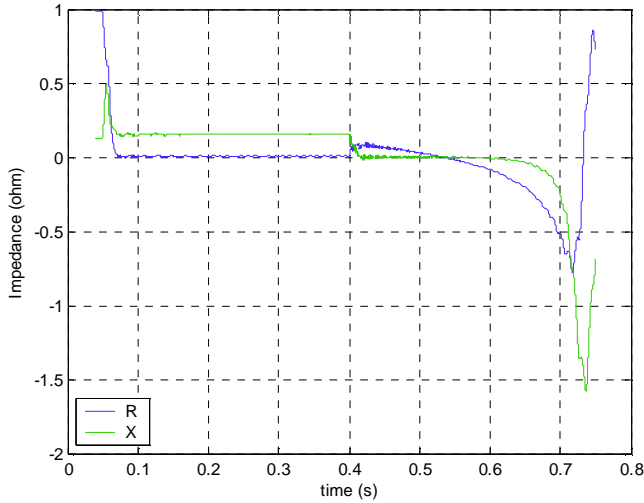


Fig. 5-2. R and X measured at the generator terminals.

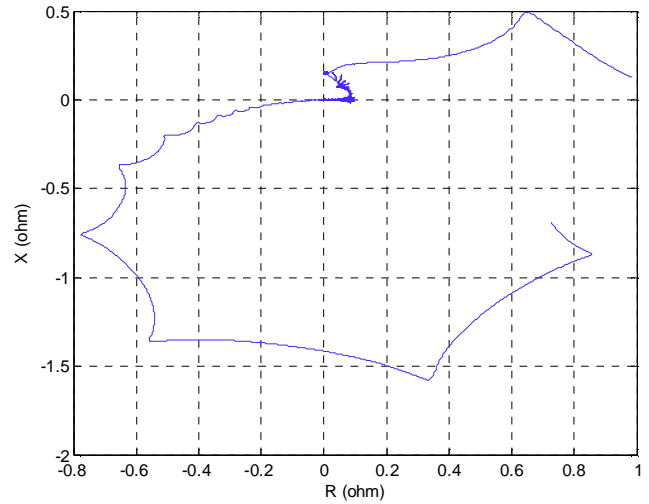


Fig. 5-3. Impedance loci.

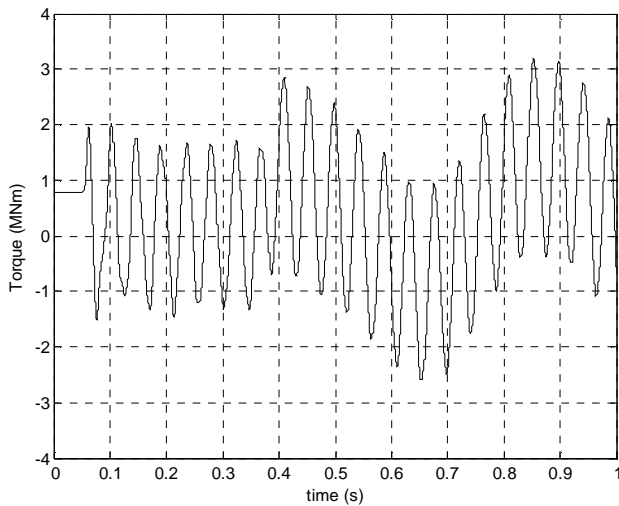


Fig. 5-4. Mechanical torque, fault cleared at $t=380$ ms

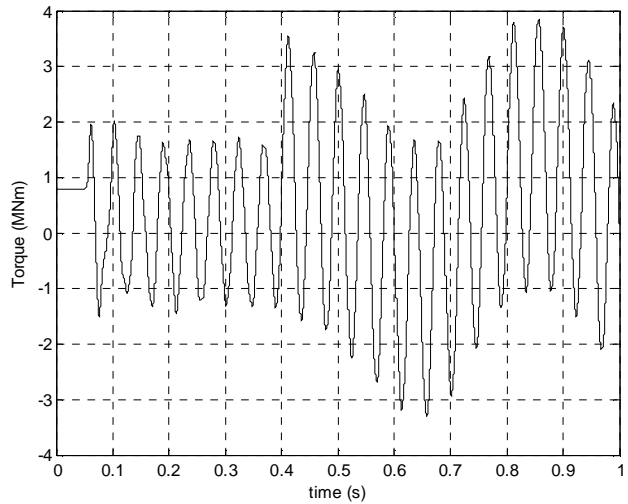


Fig. 5-5. Mechanical torque, fault cleared at $t=390$ ms

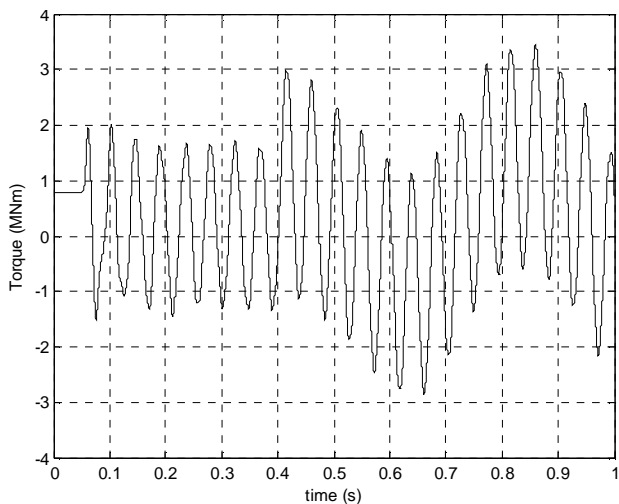


Fig. 5-6. Mechanical torque, fault cleared at $t=400$ ms

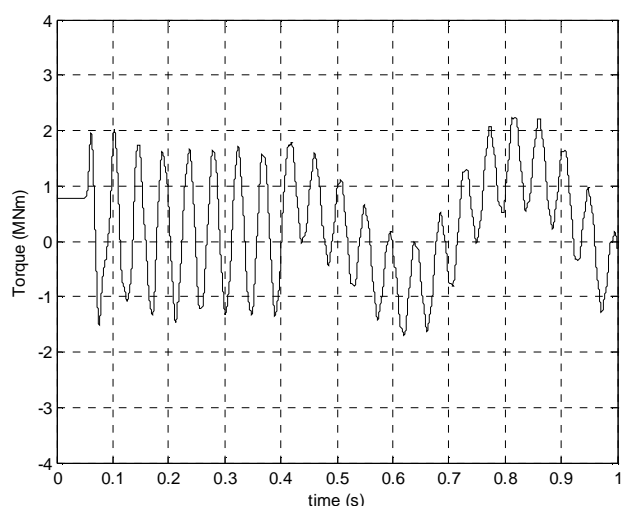


Fig. 5-7. Mechanical torque, fault cleared at $t=410$ ms

Referring to figure 3-2 for the mechanical model, figures 5-4 to 5-7 show the mechanical torque T_{or2-3} exchanged between the coupler and the turbine. Before the fault, the steady state torque assumes a constant value of 790 kNm corresponding to the 248.2 MW produced by the gas turbine.

During the fault the rotor system starts oscillating with its own modes, whose frequencies are reported in 3.2.1. After the fault clearance, the system continues oscillating with also a superimposed frequency of about 5 Hz, which is caused by the interactions among the mechanical and the electrical and control systems.

The rotating system can be considered as a torsional pendulum. The time instant of fault clearing is very important in determining the further oscillations. Actually figures 5-4 to 5-7 demonstrate that if the clearance occurs when the total (potential plus kinetic) energy is at the minimum, then oscillations are limited like in figure 5-7. Otherwise if the clearance occurs when the energy and the torque are close to their peak value, like in figure 5-5, then the oscillations reach very high values. The following table reports the torque peak values significantly variable for little variations of the clearance time (10 ms):

Clearance time (s)	0.380	0.390	0.400	0.410
$T_{or2-3_{peak}}$ (MNm)	3.1	3.8	3.2	2.2

Referring to point 3.2.2, the maximum admissible torque value for the coupler should be about 3.4 MNm, so that the instant of fault clearance is very important for the life of the mechanical system, but this instant can not be known or affected by the power plant operator, because it depends on the protection system of the HV grid.

The oscillations produce also mechanical fatigue of the rotor which can crack due to micro cracks on its surface.

6 Fault clearance at $t = 0.4$ s

The fault clearance at $t = 0.4$ s has been chosen because it is neither the best nor the worst condition. Since the torsional torque is proportional to the angular position, figure 5-6 gives an indication also of the potential energy of the “pendulum”. The best moment to open the generator circuit breaker is at $t = 0.6385$ s, as indicated in figure 6-1. The residual oscillations are limited at a peak value of 1.1 MNm.

Small differences in the moment of CB opening produce higher residual oscillations as shown in figure 6-2.

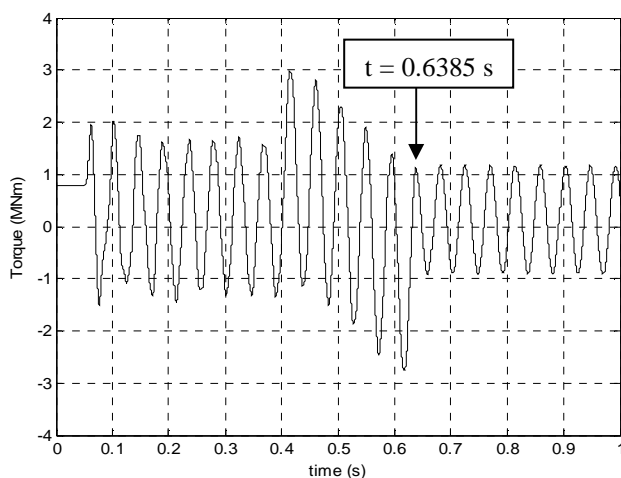


Fig. 6-1. Torsional torque, generator CB opened at $t=638.5$ ms

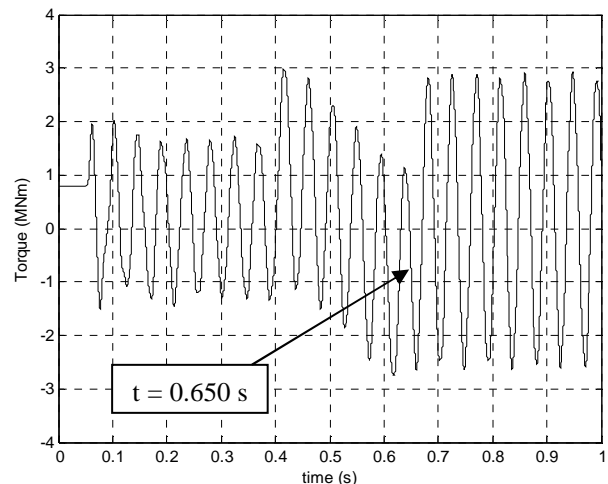


Fig. 6-2. Torsional torque, generator CB opened at $t=650$ ms

Considering a delay of circuit breaker opening of 50 ms and no further intentional delay, the sequence of events shall be as reported in the following table:

Event	Time (s)
3ph fault at 50% of the line	0.05
Fault clearance on HV side	0.4
Relay trip	0.5885
Circuit Breaker trip	0.6385

The angular displacements among rotating masses cause the torsional efforts of figure 6-3.

The opening at about 0.64 s has been determined in order to reduce the torsional efforts of the shaft. From this mechanical point of view, the generator circuit breaker (CB) must be opened as soon as possible. But this choice implies that the voltages at the circuit breaker terminals are almost in phase opposition, causing extremely high transient recovery voltages. From the electrical point of view, the CB opening should be delayed until the voltages are almost in phase again. Thus the protection setting should take into account both aspects. In this work only the mechanical aspect has been investigated.

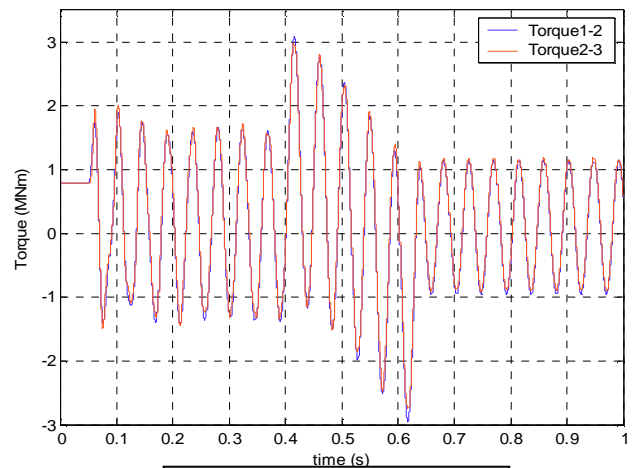


Figure 6-3. Torsional torques

6.1 Behaviour with single blinder characteristic

As already said, this is one of the simplest characteristics, defined only by two points (A and B) and a parameter (q), which determines the position of the blinder. In order to achieve an opening of the generator circuit breaker at the desired moment, the q parameter has been set at 1.8. The impedance loci of figure 6-4 describe the phenomena. After the fault has occurred, the electrical centre quickly moves towards the segment AB, where it describes a spiral, shown in figure 6-5.

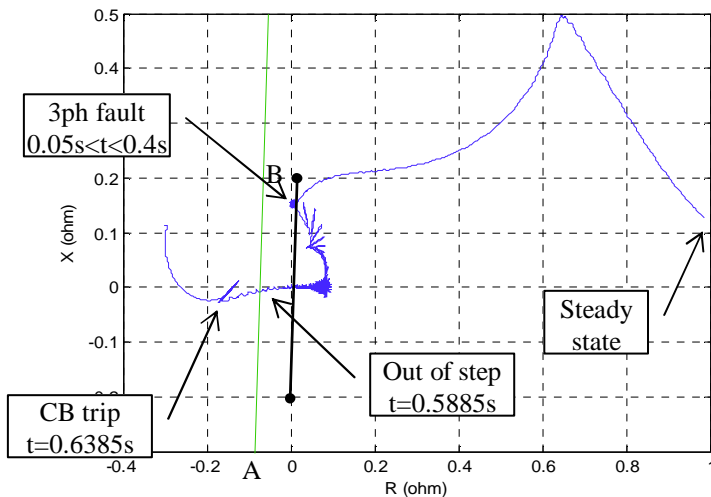


Figure 6-4. Impedance loci for $q=1.8$

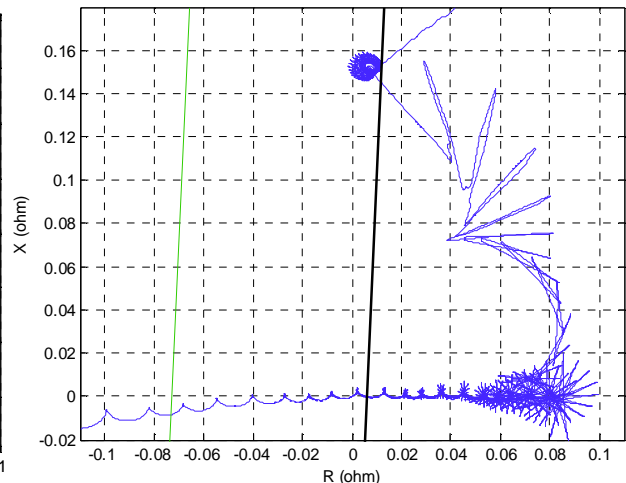


Figure 6-5. Zoom on the fault condition.

6.2 Behaviour with lens shape and tomato shape characteristics

Setting the angle of the lens shape characteristic at 140° , the CB trips at about 0.6385s (0.6366 s exactly), with torque oscillations quite similar to those shown in figure 6-3.

In order to obtain the CB tripping at the desired moment with the tomato shape characteristic, the external curve must be set at 140° . The results are the same as those of figure 6-3.

7 Changing fault location

The results reported in the previous chapter regard the out of step condition caused by a fault located at the 50% of the HV line. Moreover 3ph faults located at the 25% (further from the power plant) or at the 75% (closer to the power plant) of the HV line have been analysed.

The following diagram on figure 7-1 reports the torsional torque calculated for the three different fault locations, considering the fault duration a constant.

Differences among curves are small but not negligible. Figure 7-2 shows a magnification of fig. 7-1. It may be seen that the best moment for the CB tripping is different for different fault locations. The three curves differ for the peak values and the moment of the minimum torsional energy. A good compromise could be for $t = 0.6385$ s. However the existing relay algorithms operate on the impedance loci of figure 7-3.

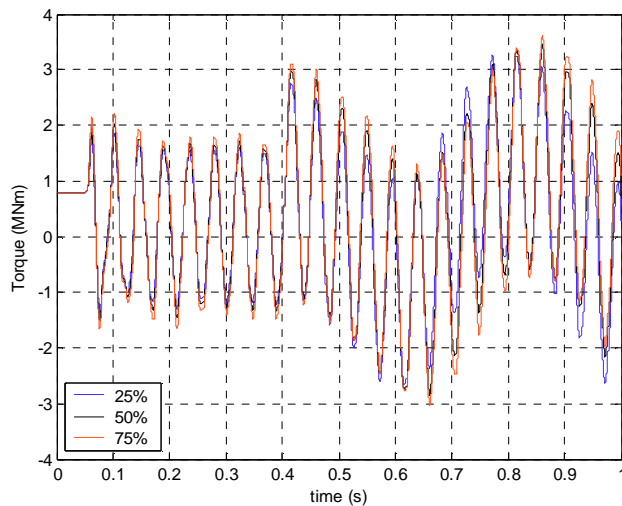


Fig. 7-1. Torque oscillations for different fault

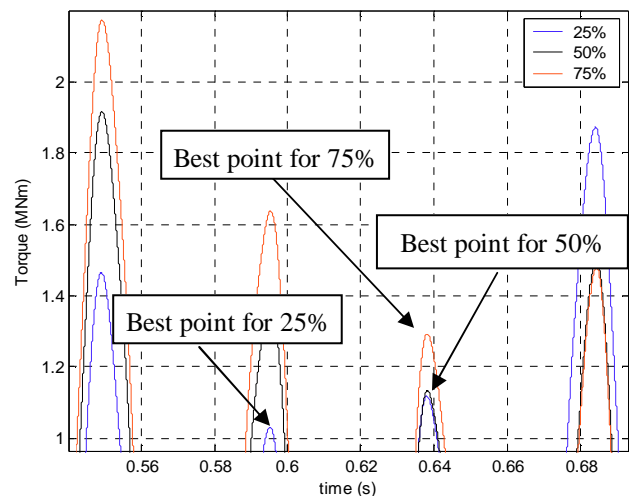


Fig. 7-2. Magnification of the torque oscillations.

Figure 7-3 shows the impedance loci for the three different fault locations. After the fault clearance, the loci have about the same path but different speeds. Actually the further the fault location is with respect to the protection, the faster the impedance loci moves. Therefore the single blinder characteristic, for example, should be able to delay or anticipate the CB trip depending on the fault distance. Otherwise setting the single blinder at $q = 1.8$, as described in 6.1, the CB opening and consequently the torque oscillations peaks vary as reported in the following table:

Fault location	25%	50%	75%
CB tripping (s)	0.6142	0.6385	0.6534
Torque peak (MNm)	2.6	1.1	2.9

These results show that the good setting found in 6.1 in case of a fault at the 50% of the HV line is no more acceptable for other fault locations.

Similar results have been obtained for lens shape and tomato shape characteristics.

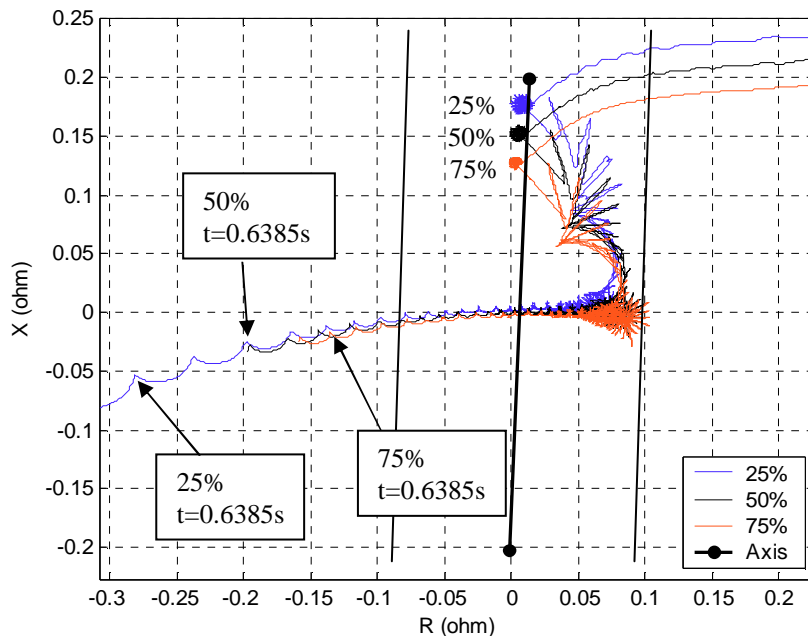


Fig. 7-3. Impedance loci for different fault locations.

8 Conclusions

The out-of-step condition of synchronous generator is cause of torsional stress for the mechanical system and electro-magnetic stress for the generator circuit breaker. The three most used algorithms of the out-of-step (78) protection have been compared. The advantages and drawbacks of single blinder, lens and tomato curves have been described and demonstrated. The single blinder and the lens shape curves are the simplest to be set, but the last one can produce unwanted trips when faults are close to one end of the protected zone. The tomato shape can produce the same results if its external curve is the same as the lens curve, but its setting requires also the calculation of the crossing time.

The results demonstrate that a protection setting should change with the fault location and adapt to the fault distance. A new generation of algorithms is therefore required to take into account not only the impedance loci but also the torsional oscillations and their consequences on the generator voltage.

9 References

- [1] ABB, "REG 316*4 Numerical Generator Protection", Doc. No. 1MRK502004-BEN.
- [2] Bacchini, "Out-of-step and power swing relaying", ABB, Doc. No. 1MRB520338.
- [3] CanAm EMTP User Group, "ATP Rule Book", 2005.
- [4] Chyn, Wu and Tsao, "Torsional fatigue of turbine generator shafts due to network faults", IEE Proc. C, Vol. 143, No. 5, pp. 479-486, 1996.
- [5] Dunlop et al., "Torsional oscillations and fatigue of steam t.g. shafts caused by system disturbances and switching events", Proc. CIGRE, 11±06, 1980.
- [6] General Electric, "LPS-O Generator Backup/Out-of-Step Protection", 2001.
- [7] Jackson, Umans, Dunlop, Horowitz and Parikh, "Turbine-generator shaft torques and fatigue - Part I: Simulation methods and fatigue analysis", IEEE Trans. on PAS, Vol. 98, No. 6, pp. 2299-2307, 1979.
- [8] Kundur, "Power system stability and control", McGraw-Hill, 1994.
- [9] Machowski et al., "Power system dynamics and stability", Wiley, 1997.
- [10] Moore K. A., "Lateral and torsional vibration study - G.E. MS9001FA model series gas turbine driving a 50Hz 324 model generator", GE Power Systems, LTR-0119-GR0729, 2001.